

## Heating and Active Control of Profiles and Transport

### by IBW in the HT-7 Tokamak

Yanping Zhao<sup>1)</sup>, Baonian Wan<sup>1)</sup>, Jiangang Li<sup>1)</sup>, Jiarong Luo<sup>1)</sup>, Junyu Zhao<sup>1)</sup>, Yuezhou Mao<sup>1)</sup>, T.Watari<sup>2)</sup>, T.Mutoh<sup>2)</sup>, Haiqing Liu<sup>1)</sup>, Yinxian Jie<sup>1)</sup>, Liquan Hu<sup>1)</sup>, Yuechun Xu<sup>1)</sup>, Jinping Qing<sup>1)</sup>, R.Kumazawa<sup>2)</sup>, T.Seki<sup>2)</sup>, HT-7 Team<sup>1)</sup>

1) Institute of Plasma Physics, Chinese Academy of Sciences P.O.Box 1126, Hefei, China

2) National Institute for Fusion Science, Toki, Gifu 509-5292, Japan

[Zhao\\_yp@mail.ipp.ac.cn](mailto:Zhao_yp@mail.ipp.ac.cn)

**Abstract:** Significant progress on Ion Bernstein Wave (IBW) heating and control of profiles has been obtained in HT-7. Both on-axis and off-axis electron heating with global peaked and local steep electron pressure profiles were realized if the position of the resonant layer was selected to be plasma far from the plasma edge region. Reduction of electron heat transport has been observed from sawtooth heat pulse propagation. Improvement of both particle and energy confinement was slight in the on-axis and considerable in the off-axis heating cases. The improved confinement in off-axis heating mode may be due to the extension of the high performance plasma volume caused by IBW. These studies demonstrate that IBWs are potentially a tool for active control of plasma profiles and transport.

### 1. Introduction

There has been a great deal of experimental work dedicated to testing the scheme of IBW for fusion plasma heating [1]. The IBW is attractive for fusion plasma heating because it has good accessibility to couple the power to the ion cyclotron resonant layer in the fusion plasma center. Nevertheless, electron Landau damping (ELD) limits the RF power available for the ions owing to the broad launched parallel wavenumber spectrum  $n_{||}$  [2]. IBW damping on electrons is further enhanced by the effect of toroidal geometry due to the oscillating property of  $n_{||}$  along the wave trajectory [3]. This effect on  $n_{||}$  can produce a localized absorption of the coupled RF power on electrons around the maxima of  $n_{||}$ . Therefore, it is attractive as a means of pressure profile control. Recent theory and experiments have shown that spatially localized IBW absorption near the resonant layer can induce a velocity shear layer, which allows suppression of electrostatic turbulence and access to a high confinement regime [4,5,6,7]. Applications of IBW could provide a degree of active external control over an internal transport barrier.

IBW heating was investigated in the HT-7 superconducting tokamak deuterium plasma [8]. The  $n_{||}$  spectrum is peaked at 8 for a frequency of 27 MHz, which is favorable for electron heating. The scheme of IBW launching and avoidance of parametric decay instability have been investigated in the HT-7 tokamak [9]. Significant progress on IBW heating has been obtained since the last IAEA meeting. IBW was explored as a tool to control profiles and transport. Both on-axis and off-axis electron heating were realized. Global peaked and local steep electron pressure profiles can be controlled by IBW. Improvement of both energy and particle confinement has been obtained.

## 2. Electron heating and pressure profiles

The electron heating mode for IBW was used for most cases in HT-7, where the electron heating was due to ELD and the ion heating mainly due to the energy transfer by electron and ion collisions [10]. In the electron heating mode, the RF frequency was 27 MHz and  $B_T$  was 1.8~2 T. Only the  $\Omega_D$  or  $2\Omega_H$  cyclotron resonant layer locates in the plasma in this case. Both global and localized electron heating was obtained. Figure 1 shows a typical discharge of global electron heating. The spatial profiles of electron temperature are shown in Fig. 2.  $B_T$  was 1.88 T, and the  $\Omega_D$  or  $2\Omega_H$  ion cyclotron resonant layer was located at a radius of 5.5 cm in the plasma center.  $I_p$  was 190 kA with  $T_e(0) \sim 1.2$  keV and  $\bar{n}_e \sim 1.1 \times 10^{13}/\text{cm}^3$  in the preheated phase. During IBW injection, the global  $T_e$  was increased to  $T_e(0) \sim 2.3$  keV, but was slightly peaked compared with the  $T_e$  profile in the target plasma. There are two possible reasons for this global electron heating. The IBW is an electrostatic wave and can intrinsically cause ELD when it propagates toward the plasma center. The  $n_{||}$  oscillates along the wave trajectory before reaching the resonant layer [11,12]. IBW absorption on electrons via ELD occurs around the maximum of  $n_{||}$  at several radial locations, which causes global electron heating. The perpendicular wavenumber  $k_{\perp}$  is strongly increased when the wave approaches to the resonant layer. The wave can strongly interact with electrons because ELD is enhanced due to the reduced wave group velocity. Therefore, RF power is further absorbed when the wave approaches the resonant layer. This localized ELD causes an increase of the central electron temperature, hence a peaked electron temperature profile. As a result, the available RF power for ion heating via cyclotron damping near the resonant layer was very limited after ELD.

The electron density was almost kept unchanged during the IBW heating phase as shown in Fig. 2. The  $H_{\alpha}/D_{\alpha}$  emission was decreased slightly, meaning an improvement of particle confinement. The global electron pressure profile shown in Fig.3 was peaked during IBW. The  $T_i(0)$  measured by a neutral particle analyzer (NPA) was also increased by about 200 eV during the IBW heating phase. The direct ion heating by IBW cannot be distinguished from electron-collision heating in the present experiments. Theory and experiments show that spatially localized IBW absorption on ions near the resonant layer can induce a velocity shear layer, which can improve the confinement [2,5]. But the available IBW power after strong ELD was insufficient to create a velocity shear over the threshold for turbulence suppression in this case, although the energy confinement time  $\tau_E$  was still slightly increased, from 8.5 ms in the target plasma to 10 ms in the IBW heated plasma.

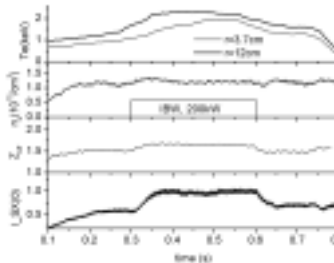


Fig.1. Shot 46882, global electron heating, IBW  $\Omega_H/2\Omega_D$  locates near the plasma center.

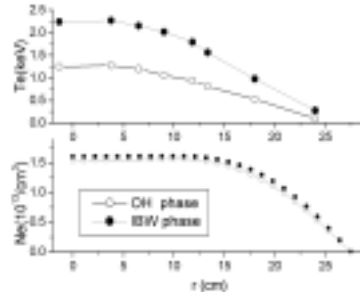


Fig. 2. Shot 46882,  $T_e$  and  $n_e$  profiles in ohmic and IBW heating phase.

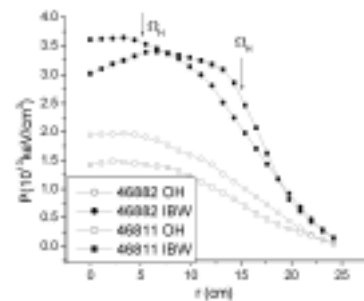


Fig. 3. Pressure profiles in ohmic and IBW heating phase for shots 46882 and 46811.

In another mode, the  $2\Omega_D$  resonant layer was near  $r \sim a/2$  for the off-axis heating, corresponding to  $B_T \sim 2$  T. Figure 4 show typical results of such a shot.  $T_e(a/2)$  exceeded  $T_e(0)$  after IBW was applied. Figure 5 shows  $T_e$  profiles. The IBW absorption via ELD due to  $n_{||}$  is not dominant because of the lower electron temperature in the out half of the plasma region. The large increase of  $T_e$  around the resonant layer is a result of reduced wave group velocity and hence enhanced ELD before the resonant layer. The remaining IBW power available for the plasma ions can induce a ponderomotive sheared flow [5], which absorbs the particles toward the resonant layer. The density is slightly increased during the IBW heated phase. This increase of density is mainly contributed from the region around the resonant layer as shown in Fig. 5, which resulted in a slightly broadened  $n_e(r)$ . As a result, the local electron pressure profile shown in Fig. 3 is steep at the region around the resonant layer in the off-axis heating mode.

### 3. Confinement and transport

The results above show that the profiles of  $T_e$  and  $n_e$  can be actively externally controlled by proper selection of plasma and IBW parameters. The IBW absorption on electrons and the power available on ions play a key role for the localized profile. This IBW scheme provides a potential means to control the localized electron pressure profile, which is needed for an advanced tokamak scenario. In both global and off-axis heating modes, particle and energy confinement is improved depending on the details of the localized pressure profiles. Detailed analysis of sawtooth heat pulse propagation shows that the electron heat diffusion coefficient was decreased.

In the global heating mode, the  $\Omega_D$  or  $2\Omega_H$  cyclotron resonant layer locates near the plasma center. Improvement of both particle and energy confinement with a peaked electron temperature profile was obtained. The degree of improvement for both particle and energy confinement is a function of the target plasma parameters and launched IBW power. Figure 6 shows a comparison of  $\tau_E$  for different injected IBW powers. The  $\tau_E$  were increased by  $\sim 10\%$  and  $20\%$  for the launched RF powers of 155 kW and 210 kW in the same target plasmas. Detailed energy balance analysis is not available in the present work. Useful information about electron energy transport can be qualitatively obtained by the peak to time analysis of the heat pulse propagation of the sawtooth (ST). Figure 7 shows ST oscillations in the preheated and IBW heated phases of the shot shown in Fig. 1. The amplitude of the

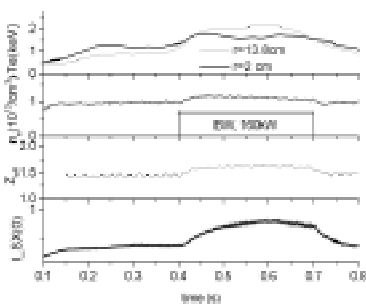


Fig. 4. Shot 46811, local electron heating, IBW  $\Omega_H/2\Omega_D$  resonant layer locates at  $r = 15.8$  cm.

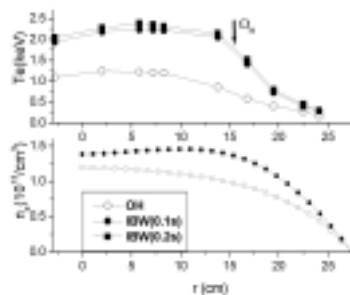


Fig. 5. Shot 46811, electron temperature and density profiles in ohmic and IBW heating phase.

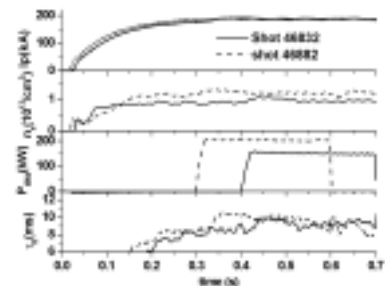


Fig. 6. Energy confinements was improved little in global IBW heated plasmas

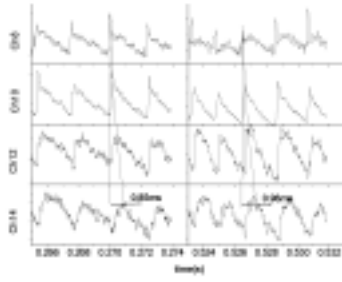


Fig. 7. Shot 46882, the delay time of the ST was prolonged from 0.85 ms in the ohmic phase to 0.96 ms in the IBW heated phase.

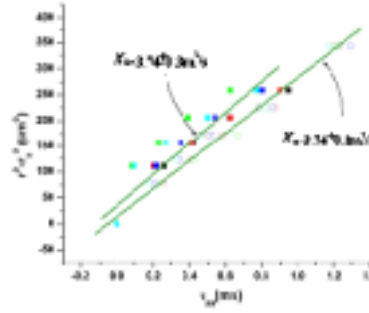


Fig. 8. Plot of differential radius squared  $r^2 - r_s^2$  versus  $\tau_{pp}$ .

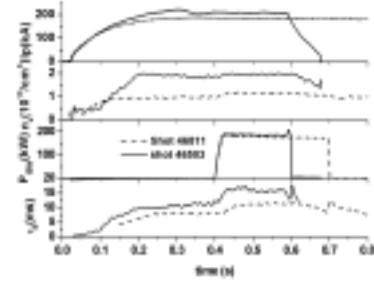


Fig. 9. Energy confinement was improved considerably in localized IBW heated plasmas

oscillations became larger in the IBW heated phase, owing to the increased electron temperature. The delay time of the oscillation peaks between the adjacent channels was prolonged, which means a reduced electron heat diffusion coefficient. Figure 8 gives the plot of radius squared versus  $\tau_{pp}$ , where  $\tau_{pp}$  is the time delay of a heat pulse from the mixing radius to the corresponding location. To a first approximation, the slope of the connected line is a measure of the electron heat diffusion coefficient at the corresponding radial extent. Obviously, the slope of the curve for the IBW heating phase is smaller than that for the preheated phase. This fact means that the electron heat diffusion coefficient was decreased in the IBW heated phase

In the off-axis heating mode, the electron pressure is strongly steepened around the resonant layer. This is owing to the larger available power for the ELD before the resonant layer, which causes a larger increment of the localized electron temperature. In this case, the energy confinement is significantly improved compared with that of the global heating mode. Figure 9 shows the energy confinement times in two different target plasmas with the same  $B_T$  and similar launched IBW powers. The  $\tau_E$  increments are  $\sim 38\%$  and  $\sim 50\%$  for shots 46811 and 46503 respectively. The target plasma parameters of shot 46811 are very close to those of shot 46882 except for the toroidal field strength. Better plasma performance in the off-axis heating mode may be a result of the extension of the high performance plasma volume. Similar characteristics of the ST oscillation were observed as in the global heating mode. A considerable reduction of the electron heat diffusion coefficient can be estimated from the sawtooth heat pulse propagation in this heating mode. The large pressure gradient as shown in Fig.3 forms an internal transport barrier-like structure at the position around the resonant layer. A further detailed study is needed to clarify whether this ITB-like profile can account for the improved confinement.

#### 4. Discussion and conclusion

The electron heating mode for IBW was used in HT-7, where the electron heating was due to electron Landau damping at the maximum of the launched  $n_{||}$  spectrum and before the resonant layer. Both global and localized electron heating were obtained by locating the resonant layer in the plasma far from the edge region. Bulk ion heating was the original motivation of the IBW heating scheme. More recently, theoretical and experimental results showed that IBW absorbed on ions can produce a ponderomotive sheared flow and therefore

can be used to suppress turbulence and improve confinement. This ponderomotive force by IBW induces a density absorption into the sheared layer and causes a localized density increase around the ion resonant layer. This feature could be used to control the plasma electron pressure profiles, if the plasma target and the launched IBW  $n_{||}$  were properly arranged. In the global heating mode, a peaked electron pressure profile was obtained in the HT-7 tokamak when the ion cyclotron resonant layer was put close to the plasma center. The localized electron pressure profile is steep at the region around the resonant layer in the off-axis heating mode. These operation modes provide a potential means to control the localized electron pressure profile, which is needed for an advanced tokamak scenario. In these modes, both particle and energy confinement was improved. Analysis of sawtooth heat pulse propagation shows that the electron heat diffusion coefficient is decreased slightly in the global heating mode and significantly in the off-axis heating mode. An ITB-like electron pressure formed in the off-axis heating mode opens the possibility of its use for active transport control.

### Acknowledgements

This work was supported by the National Natural Science Foundation of China under Grant No. 10175069.

### Reference

- [1] M.Ono, Phys. Fluids **B5**, 241 (1993).
- [2] A.Cardinali, C.Castaldo, R.Cesario, F.De Marco, F.Paoletti, Nucl. Fusion **42** 427 (2002).
- [3] A.Cardinali, F.Romanelli, Phys. Fluids **B4** 504 (1992).
- [4] L.A.Berry, E.F.Jaeger, D.B.Batchelor, Phys. Rev. Lett. **82** 1871 (1999).
- [5] E.F.Jaeger, L.A.Berry, D.B.Batchelor, Phys. Plasmas **7** 3319 (2000).
- [6] B.LeBlanc et al., Phys. Rev. Lett. **82** 331 (1999).
- [7] K.H.Burrell, Phys. Plasmas **6** 4418 (1999).
- [8] Y.P.Zhao et al., Plasma Phys. Control. Fusion **43** 343 (2001).
- [9] J.Li et al., Plasma Phys. Control. Fusion **43** 1227 (2001).
- [10] B.N.Wan et al., "PSI Issues toward Steady State Plasmas in the HT-7 Tokamak", 15<sup>th</sup> PSI, I-11, May 27-31 2002, Gifu, Japan.
- [11] F.Paoletti et al., Phys. Plasmas **6** 863, (1999).